WAKEFIELD STUDIES OF IVUE32

P. Volz*, A. Meseck, S. Grimmer,
Helmholtz-Zentrum Berlin für Materialien und Energie, Berlin, Germany

Abstract

The Helmhotz-Zentrum Berlin (HZB) is developing an elliptical in-vacuum undulator, IVUE32, following the APPLE-II design with a magnetic force compensation concept. The undulator will be installed in the BESSY II storage ring. It will feature a 7 mm minimum gap and four magnet rows that can be moved to adjust the polarization of the synchrotron radiation. This shift movement requires a complex taper structure and a longitudinal slit in the shielding foils. Extensive CST wakefield simulations have been conducted to investigate the interaction between the undulator and the beam. The impedance of the device on the beam is studied, as well as the heating of the undulator induced by the beam. The taper structure has to compensate for two axes of motion. The vertical gap movement and the longitudinal shift movement. The shift movement is different for each half of the shielding foil. Previously presented designs used separate foil tensioning systems to independently compensate for the two axes of motion. A length constraint due to the β-function might prohibit the separate compensation. Changing the gap while also compensating for the shift motion introduces an asymmetry in the taper, where the shielding foils have different gradients. Different asymmetric tapers are studied to find the limits for horizontal impedance for the BESSY II beam.

INTRODUCTION

The APPLE II design of IVUE32 [1] as an in vacuum undulator poses several challenges for beam dynamics. Compensation of the two axes of motion requires a complex taper and a longitudinal slit in the shielding foils. These components can cause resonances in impedance, disrupting beam dynamics and heating components. Their impact needs to be investigated before such a device can be installed into the storage ring. We present extensive simulations of possible taper designs and their impact on impedance. As well as studies of possible deviations of shielding foil geometry and the expected heat load.

IVUE32 TAPER SIMULATIONS

Wakefield simulations using the CST Studio Suite Software [2] of the IVUE32 taper structure have been conducted. The taper structure is modeled inside a cylindrical vacuum chamber with a diameter of 40 cm to mimic the vacuum chamber of IVUE32. Earlier design iterations featured an electrical discontinuity in order to preserve vacuum quality. This causes unacceptably high impedance [3], leading to a design with two foil tensioning mechanisms [3]. This design fully separates the gap movement compensation and shift movement compensation, avoiding possible transverse asymmetries due to a compound taper. The detailed simulations of this taper design were not ready for last year's IPAC and are shown in Fig. 1. The longitudinal impedance

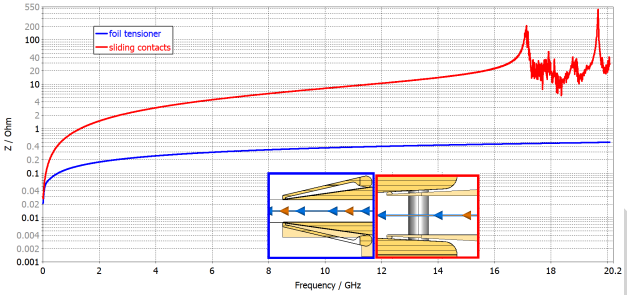

Figure 1: Longitudinal impedance of IVUE32 shift movement compensation at a gap of 7 mm. Sliding contact design (red) compared to foil tensioner design (blue)

of the shift compensation mechanism at a gap of 7 mm is compared to an earlier design with sliding contacts. The foil tensioning mechanism features a very smooth geometry without any significant changes in gap. The sliding contacts of the earlier design cause a 1 mm step in the gap, followed by a small taper. Therefore the foil tensioning design has a lower impedance across the whole spectrum and does not show any resonant frequencies.

The IVUE32 magnet structure will have a length of 2.5 m. The β-function with the current beam optic at the designated straight section can only support the planned minimum gap of 7 mm for about that distance. The foil-tensioner shift-compensation mechanism would maintain the gap of the magnet structure for about 30 cm at either side of the undulator, making it incompatible with the current beam optic. Therefore a compound gap and shift taper that immediately increases the gap from 7.4 mm at the magnet girder to 9 mm is studied. This compound taper introduces transverse asymmetries to the gap geometry that change with the shift state, similar to the case discussed in [3] but with a much lower magnitude. The aim of this simulation study was to find an acceptable compromise between impedance impact and immediate gap increase. Both the gap compensation and shift compensation are modeled as simplified copper foils. Figure 2 shows the compound taper at different shift states from the side with the asymmetry highlighted in red. The vertical axis is exaggerated to better visualize the geometry. The taper connects to the magnet girders at the right with a gap of 7.4 mm. The gap in the shift compensation section increases through various tapers dictated by the foil mounting points and magnet infrastructure to 9 mm. The shielding foil in this section is split longitudinally. This causes a slight asymmetry between the two halves of the foil, highlighted in red, the geometry of which changes with shift movements.

* paul.volz@helmholtz-berlin.de

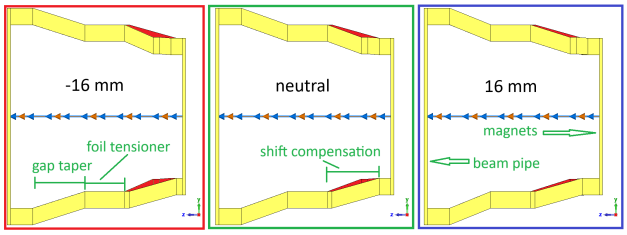

Figure 2: Side view of the compound taper model at shift states of −16 mm, neutral and 16 mm. Exaggerated vertical axis with asymmetries highlighted in red.

The foil tensioner section and gap taper do not have a longitudinal slit and their geometry does not change with shift movements of the undulator. The gap taper connects to the beam pipe of the accelerator, which has a gap of 11 mm.

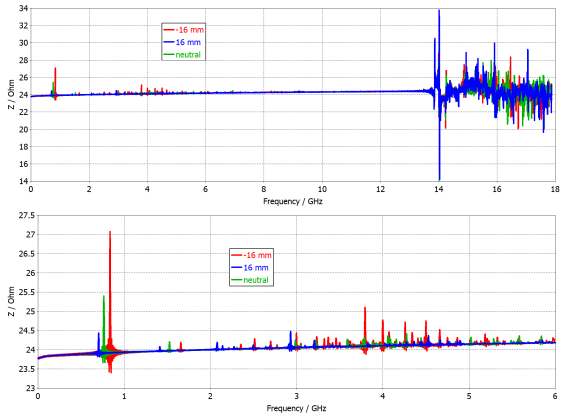

Figure 3: Longitudinal impedance of the compound taper shown in Fig. 2. Full spectral range at the top, low frequency excerpt at the bottom.

Figure 3 shows the longitudinal impedance of the compound taper shown in Fig. 2 for the three shift states. Below 14 GHz the impedance shows a few peaks, hinting at resonances in the taper geometry. The most notable peak is just below 1 GHz. This peak moves slightly in frequency and changes amplitude with the shift state of the undulator. The shift state of −16 mm shows the largest amplitude with an impedance of 27 Ω. Please note that the impedance does not drop close to 0 Ω in the DC limit. This is an artifact due to the aperture mismatch [4] in the simulation, which models only part of the device. Considering this , the relative magnitude of the worst resonance is only 3 Ω.
Further investigation into the impedance contribution of the whole structure of IVUE32 is needed to make a final decision but the simulated compound taper would fit into the impedance budget.

FOIL SLIT SIMULATIONS

The APPLE-II design of IVUE32 calls for a longitudinal slit in the magnet shielding foils. To fully shield the permanent magnets from the electron beam and possible upstream synchrotron radiation, it is planned to fold the shielding foil into the gap between the magnet girders as shown in Fig. 4.

This is a novel design, requiring intensive investigation into impedance and heating behavior before implementation.

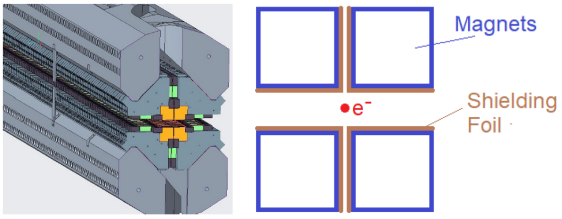

Figure 4: CAD model of IVUE32 magnet girders on the left and schematic of folded magnet shielding foils on the right.

Slit Deviations

To investigate the effects of possible deviation in slit geometry caused by the folding of the shielding foil, two types of errors are investigated. The first type of error is a sinusoidal deviation of the foil slit, while keeping the width of the slit constant. The second type of error is a symmetric variation of the slit width. The geometry of these two types of deviation is shown in Fig. 6 together with the density of surface current induced by the passing beam. Preliminary results were presented earlier [5], here we present the detailed impedance impact of these shielding foil slit deviations. A 1 m section of shielding foils is simulated with the CST wakefield environment. As with the taper, the foils are simulated inside a cylindrical vacuum chamber with a diameter of 40 cm to closer resemble the actual undulator. After 20 mm of solid foils a longitudinal slit is introduced. The slit starts at the center of the foil at a width of 1 mm. Depending on the type of deviation investigated, the width or slit position varies for the subsequent 960 mm. For the last 20 mm the foil is modeled without a slit. The slit is mirrored on the opposite foil. To save simulation time, a magnetic symmetry is defined at the xz-plane.

Figure 5 shows the longitudinal impedance of the two

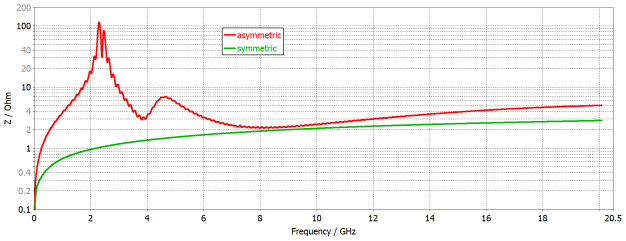

Figure 5: Longitudinal impedance of the two different types of foil slit deviations depicted in Fig. 6.

different types of foil slit deviations. The sinusoidal deviation (marked in red as *asymmetric*) shows a much higher impedance with distinct resonant peaks. The symmetric slit width variation (marked in green as *symmetric*) shows a much lower impedance across the whole frequency range without any resonant peaks.
Figure 6 shows the surface currents induced by the electron beam passing from left to right. The sinusoidal deviation clearly shows a significant trail of surface currents after

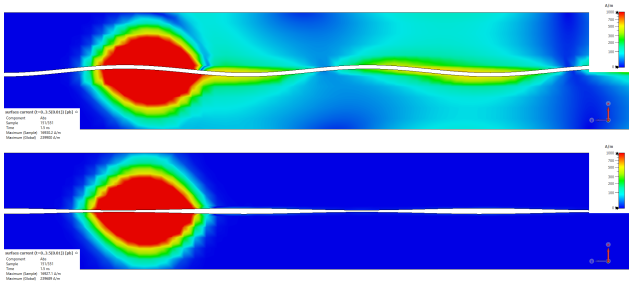

Figure 6: Surface current distribution on the IVUE32 shielding foil for different types of slit geometry deviations. Sinusoidal deviation at the top, symmetric gap width deviation at the bottom.

the mirror charge induced by the passing beam. These correspond to the resonances shown by the impedance. The symmetric slit width deviation show no significant surface currents in the foils after the passing beam.
As a rough estimation we consider the shielding foils a rectangular waveguide and the sinusoidal slit deviation as a perturbation in the form of a rectangular cavity. Resonant modes are given by

$$f_{nml} = \frac{c}{2}\sqrt{\left(\frac{n}{x}\right)^2 + \left(\frac{m}{y}\right)^2 + \left(\frac{l}{z}\right)^2} \qquad (1)$$

with c the speed of light and x, y, z the respective dimensions. With $z = 62.8\,\text{mm}$ as the period length of the sinusoidal deviation, $f_{001} = 2.39\,\text{GHz}$ matches the resonance shown in Fig. 5 well. The first harmonic $f_{002} = 4.77\,\text{GHz}$ is visible with a much smaller amplitude.

Power Loss

The shielding foils consist of a copper layer with a thickness in the order of 50 µm laminated with a nickel layer that provides ferromagnetic attraction to the permanent magnets. These thin foils need to carry the current of the mirror charge induced by the passing beam. This causes heating due to their finite conductivity. It is important to determine the heat load on the shielding foils in order to design adequate cooling and prevent damage to the shielding foils and permanent magnets.
The CST wakefield solver can determine the power loss for simulated components. A section of foil is simulated for the beam parameters of the BESSY II standard user fill pattern [6] . Figure 7 shows the power over time that the foil segment receives from the different passing beams.
These power curves are integrated to gain the deposited energy. Higher charge bunches like the single bunch and the PPRE bunch deposit more energy than the lower charge standard user bunch. This is then weighed with the length of the simulated segment and the BESSY II fill pattern to get the total heat load on the shielding foils over the length of IVUE32. This comes out to 16.1 W distributed over a length of 2.5 m. This might not sound dramatic but it is significant heating in the context of an enclosed vacuum environment. The source of the heat load are the induced surface currents.

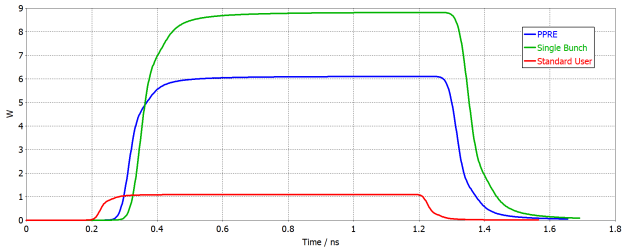

Figure 7: Power loss of the IVUE32 copper shielding foils for different bunches from the BESSY II standard user fill pattern [6].

The heat load distribution is therefore proportional to the surface current density. Figure 8 shows that density for a perfectly straight slit. It is concentrated on the folded edge of the shielding foil and does not reach far into the slit between the magnet girders.

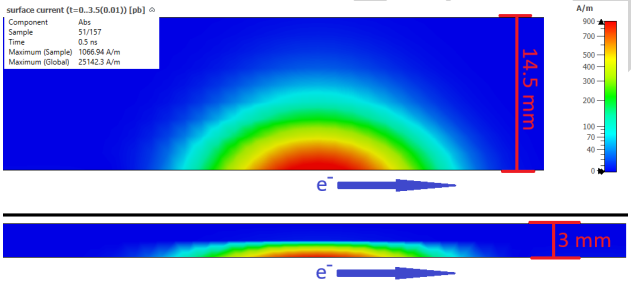

Figure 8: Surface current distribution on the IVUE32 shielding foil. Horizontal distribution shown at the top, vertical distribution shown at the bottom.

The only possible cooling of the thin shielding foils comes through the contact with the permanent magnets. The folded edge where the heat load is concentrated is unfortunately the most likely point for the shielding foils to lose contact with the magnets acting as a heat sink. Heating the foils causes thermal expansion and further detaching from the heat sink. This avalanche failure [7] can melt the foils, causing catastrophic damage to the undulator.
The foil heating will be further investigated with thermal simulations and in vacuum test stands.

CONCLUSION AND OUTLOOK

After extensive simulations and many design iterations we have arrived at a taper design that can compensate the complex motion of IVUE32 with minimal impact on the beam impedance. Even the added β-function constraints could be solved with a compound taper that still fits in the impedance budget.
Investigations of the shielding foil slit show potential sources of resonant impedance. Precision manufacturing however, will produce deviation amplitudes far smaller than what is needed to significantly impact impedance.
One remaining concern is the concentration of the heat loss at the folded edge of the shielding foils. Thermal simulations and experimental set ups will determine the required cooling infrastructure.

REFERENCES

[1] J. Bahrdt *et al.*, "In-Vacuum APPLE II Undulator", in *Proc. 9th International Particle Accelerator Conference (IPAC'18), Vancouver, BC, Canada, April 29-May 4, 2018*, Vancouver, BC, Canada, pp. 4114–4116, Jun. 2018. doi:10.18429/JACoW-IPAC2018-THPMF031

[2] Dassault Systèmes, "Dassault Systèmes SIMULIA CST Studio Suite", www.3ds.com/products-services/simulia/products/cst-studio-suite,

[3] P. Volz, A. Meseck, and S. Grimmer, "Wakefield Studies of the Taper Section of the Elliptical In-Vacuum undulator - IVUE32", in *Proc. IPAC'25*, Taipei, Taiwan, Jun. 2025, pp. 1591–1594. doi:10.18429/JACoW-IPAC2025-TUPS092

[4] G. Stupakov, "Low Frequency Impedance of Tapered Transitions with Arbitrary Cross Sections", *Phys. Rev. ST Accel. Beams*, vol. 10, no. 9, p. 094401, Sep. 2007. doi:10.1103/PhysRevSTAB.10.094401

[5] P. Volz and A. Meseck, "Loss Simulations on Shielding Foil Slit Errors", in *Proc. IPAC'23*, Venice, Italy, pp. 3494–3497, May 2023. doi:10.18429/JACoW-IPAC2023-WEPL160

[6] "Operating Modi BESSY II", https://www.helmholtz-berlin.de/forschung/oe/be/operation-accelerator/betriebsmodi_en.html, Accessed: 2026-05-09,

[7] J.-C. Huang, H. Kitamura, C.-H. Chang, C.-H. Chang, and C.-S. Hwang, "Beam-Induced Heat Load in In-Vacuum Undulators with a Small Magnetic Gap", *Nuclear Instruments and Methods in Physics Research Section A: Accelerators, Spectrometers, Detectors and Associated Equipment*, vol. 775, pp. 162–167, 2015. doi:10.1016/j.nima.2014.11.116